Obstacle Avoidance Model for UAVs with Joint Target based on Multi-Strategies and Follow-up Vector Field

Xue Zheng, Stéphane Galland, Xiaowei Tu, Qinghua Yang, Alexandre Lombard, Nicolas Gaud

Available online at www.sciencedirect.com

ScienceDirect

Procedia Computer Science 00 (2019) 000–000

Procedia Computer Science

www.elsevier.com/locate/procedia

The 11th International Conference on Ambient Systems, Networks and Technologies (ANT)
April 6 - 9, 2020, Warsaw, Poland

Obstacle Avoidance Model for UAVs with Joint Target based on Multi-Strategies and Follow-up Vector Field

Xue Zheng[a], Stéphane Galland[b,*], Xiaowei Tu[a], Qinghua Yang[a], Alexandre Lombard[b], Nicolas Gaud[b]

[a]*Department of Mechatronic Engineering and Automation, Shanghai University, 200072, Shanghai, P.R. China*
[b]*CIAD, Univ. Bourgogne Franche-Comté, UTBM, F-90010 Belfort, France*

Abstract

A multi-strategies obstacle avoidance method based on follow-up rotating vector field is proposed for UAV flight planning. The inter-UAVs repulsion with distance factor and the target directional gravity are used as the inter-UAVs control strategy. In the process of obstacle avoidance, the artificial potential field method is used outside the obstacle to guide the UAVs to sail to the target point. In the obstacle avoidance scope, the follow-up rotating vector field method is proposed to avoid convex polyhedral obstacles. Finally, smoothing strategy is conbined to the follow-up rotating vector field to obtain safety and smoothing path. The simulation results show that the proposed algorithm can solve the problem of "dead zone" and "jitter" in the track by combining various strategies, and realize the obstacle avoidance behavior while avoiding collision between machines.

Keywords: track planning; follow-up rotating vector field; multi-strategies obstacle avoidance

1. Introduction

Unmanned Aerial Vehicles (UAVs), most commonly known as UAVs, are becoming increasingly popular for civilian applications in several domains such as agriculture, transportation, products delivery, energy, emergency response, telecommunication, environment preservation and infrastructure. According to Teal Group's 2018 World civilian UAV Market Profile and Forecast report [11], civilian UAV production will total US$88.3 billion in the next decade, with a 12.9% compound annual growth rate. In this context, regulation and collision avoidance are among the prominent challenges to be settled [9].

*Corresponding author. S. Galland; Tel.: +33 384 583 418.
E-mail address: stephane.galland@utbm.fr

There are many ways to realize obstacle avoidance and path planning for a single UAV, such as A*-like algorithm [7, 12], social force models [5, 10, 3], artificial potential field method [6], or velocity spaces [1, 4]. Among these different approaches, the artificial potential field method is a virtual force method proposed by Lewin [8] and applied to agent navigation by Helbing and Molnar [5] and Reynolds [10]. Its basic idea is to design the robot's movement in the surrounding environment as an abstract movement in the artificial gravity field. The target point produces "attraction" to the mobile robot, and the obstacle produces "repulsion" to the mobile robot. Finally, the movement of the mobile robot is controlled by seeking the resultant force. Several problems may occur with this approach: 1. definition of the attraction term of the force; 2. determination of the application point of a repulsive force on a complex shaped obstacle; 3. definition of the scale of the repulsive forces. These issues may leads to trajectories that are not smooth, or that are not avoiding collisions at all (especially in a high density environment).

In this paper, we consider the case in which all UAV have to reach the same target position. In order to avoid the previously mentioned issues in this context, a follow-up rotation vector field applied in obstacle avoidance is proposed. It combines the improved artificial potential field method to realize the path planning of UAV in complex environment. Under the conditions of many kinds of convex polyhedron environment modeling, combined with the multi strategy methods such as collision avoidance between aircraft, follow-up rotation vector field, smoothing strategy and so on, the better path planning of UAV can be realized.

The paper is structured as follow. Section 3 present the obstacle avoidance model that is used by the UAVs. Section 4 provides details on two strategies that may be used for applied the proposed collision avoidance model. An experimental validation of the proposed model is presented and discussed in Section 5.

2. Background

The analytical model for microscopic model (for pedestrian and applied recently to UAV) has been developed by Helbing and Molnar [5], but the numerical solution of the model is very difficult to obtain, and simulation is more practical and favorable. Reynolds [10] proposes to build pedestrian models from a collection of "steering behaviors" that is also considered as a possible solution for drones. One of the key points in the motion of UAVs is to avoid collision with the other UAVs and with the obstacles. The models inheriting from the force-based model of Reynolds [10] are able to avoid collisions. Unfortunately, the trajectories of the UAVs differ from optimal ones. This is due to the lack of collision prediction and anticipation of the other UAVs motions. Predictive and cooperative models, especially for pedestrians are proposed to avoid collisions [2]. Treuille et al. [13] proposes a dynamic potential field that simultaneously integrates global navigation and moving obstacles such as other UAVs, efficiently solving the problem of the motion of large population without the need for explicit collision avoidance.In addition,The traditional artificial potential field obstacle avoidance model has the problem of dead zone[14], when the UAV, obstacles and target point are in a straight line,and Obstacles are located between UAV and target terminal.Since Obstacles has lower attractive potential, the robot will move to the direction of the target point. Then, the repulsive force of obstacles becomes stronger, and the robot cannot go to the goal which is the global minimum point but stays at the local minimum point called the local well.

3. Individual Obstacle Avoidance Model

3.1. Obstacle Model

There are many obstacles in the three-dimensional environment. Because the shape of some obstacles is irregular and difficult to deal with directly, they are replaced by convex polyhedron obstacles such as spheres, ellipsoids and cuboids to better modeling.The obstacles' model uses a uniform expression:

$$\Omega(\rho_i) = \left(\frac{x_i - x_0}{a}\right)^2 \left(\frac{y_i - y_0}{b}\right)^2 \left(\frac{z_i - z_0}{c}\right)^2 \tag{1}$$

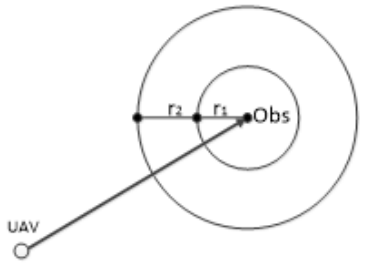

Fig. 1. The relation between UAV and obstacle

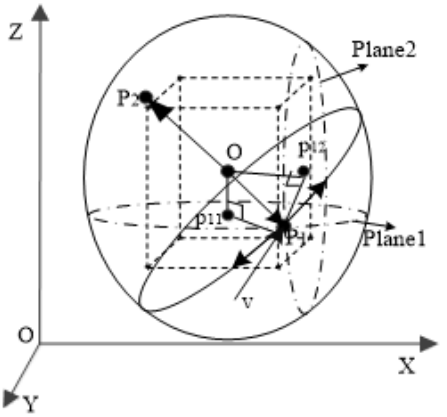

Fig. 2. Follow-up rotating vector field

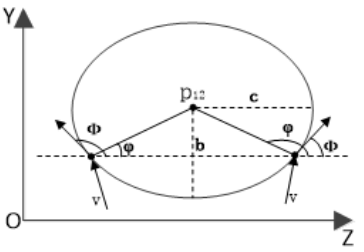

Fig. 3. Rotating vector field in *zoy* plane

Where (x_0, y_0, z_0) indicates the three-dimensional position of the obstacle center, $\rho_i = (x_i, y_i, z_i)$ is the three-dimensional position of the i-th UAV in the global coordinate system. The coefficient a, b, c determine the size and shape of the obstacle. The sphere or ellipsoid can be obtained by combining different coefficients. When the obstacle is represented as a sphere, then $a = b$. $\Omega(o) > 1$ indicates the outside of the obstacle, $\Omega(o) < 1$ indicates the inside of the obstacle, and $\Omega(o) = 1$ indicates the surface of the obstacle. Therefore, the no-fly zone or the danger zone is represented by the inside and the surface of the convex polyhedron:

$$\mathrm{R}^{\Omega}(\rho_i) = \{\rho_i | \Omega(\rho_i) \leq 1\} \tag{2}$$

In the actual track planning, due to the interference of various external factors, in order to ensure the planning of a safe track, a safe distance is added around the obstacle. As shown in Fig. 1, where r_1 is the radius of the obstacle interface, r_2 is the safe distance, and $a = r1 + r2$ is the shape coefficient of the obstacle. Therefore, in the following research, when the distance between UAV and obstacles should be greater than 0, it is considered that obstacle avoidance is successful.

3.2. Follow-up Rotating Field

The problem of obstacle avoidance can be explained as the situation where the UAV does not enter the danger zone, and autonomously navigates around the obstacle and reaches the end point. It means that there must be a continuous point set around the obstacle that satisfies the condition $\rho_i \notin \mathrm{R}^{\Omega}(\rho_i)$ so that the UAV can move around the obstacle.

Accordingly, in order to obtain a continuous and smooth track with collision avoidance, a follow-up rotating vector field is introduced. As shown in Fig. 2, the urban building is regarded as a cuboid, and the obstacle model is established as ellipsoid according to the size of the cuboid and the obstacle model in Equations 1 and 2. In the process of obstacle avoidance, the UAV is always subjected to two vector fields from the *xoy* plane and the *zoy* plane. In order to avoid obstacles better, three-dimensional obstacle avoidance is transformed into a combination of two-dimensional plane obstacle avoidance. Based on the morphing artificial potential field function introducing stream method used for obstacle avoidance, the follow-up rotating field enables UAVs to avoid around obstacles in a streamline way to eliminate deadzone problems.

The two vector fields are formed by the relative positions of the UAV and the obstacle, so they will follow the position change of the UAV and the obstacle. When the UAV moves from p_1 to p_2, different rotating vector fields will re-form. When the UAV enters the obstacle avoidance zone $P1$ (Fig. 2) at a speed v, an ellipsoid or sphere spatial structure is constructed with the distance between the current position of the UAV and the center position of the obstacle. When the plane 1 contains the $P1$ point and is parallel to the plane *xoy*, the radius is P_1p_{11}, and p_{11} is the

vertical point of the obstacle center O on the plane 1. When plane 2 contains the point $P1$ and is parallel to the plane zoy, the radius is P_1p_{12}, and p_{12} is the vertical point of the obstacle center O on plane 2. The unit direction vector of the relative distance between $P1$ and the obstacle is $E = \left(\frac{X_0-X_i}{r}, \frac{y_0-y_i}{r}, \frac{z_0-z_i}{r}\right)$. r is the relative distance between the UAV and the obstacle. The radial normal vector of the sphere is $n = \left(\frac{\delta\Omega}{\delta x}, \frac{\delta\Omega}{\delta y}, \frac{\delta\Omega}{\delta z}\right)$.

The analysis of vector field in zoy plane is also shown on Fig. 3. Its principle is the same for xoy plane. When the obstacle is shaped like a cylinder or a cuboid, an elliptical vector field is formed between the UAV and the obstacle in the zoy plane. As shown on Fig. 3, φ is the angle between the vector field and the z axis , ϕ is the angle between the relative position of the obstacle and the UAV and the z axis. The direction of φ and ϕ is determined according to different angles of the UAV entrying rotating field. According to the definition of the obstacle of Equation 3, the matrix of the follower vector field between the obstacle and the UAV in the zoy plane can be obtained:

$$M_i^{zoy} = \begin{cases} \left[0, -\frac{c}{b}(y_0 - y_i), \frac{b}{c}(z_0 - z_i)\right] & \text{if } \varphi < \phi \text{ (anticlockwise)} \\ \left[0, \frac{c}{b}(y_0 - y_i), -\frac{b}{c}(z_0 - z_i)\right] & \text{if } \varphi > \phi \text{ (clockwise)} \end{cases} \tag{3}$$

The UAV is subject to the attraction of the target direction before entering the vector field. Consequently, the angle between the direction of the UAV entering the rotating vector field and the direction of the target's attraction is assumed to be small. To achieve a shorter reach of the target and reduce the major mobile effect, the direction of the vector field is determined by the comparison between the angle φ of current vector field and the angle ϕ of the relative position between the obstacle and the UAV. The direction of the vector field is defined by: $\varphi < \phi$, when the vector field direction is counterclockwise; or $\varphi > \phi$, when the vector field direction is clockwise.

Similarly, in the xoy plane, the vector field matrix of obstacle and UAV can be obtained:

$$M_i^{xoy} = \begin{cases} \left[\frac{b}{a}(x_0 - x_i), -\frac{a}{b}(y_0 - y_i), 0\right] & \text{if } \gamma < \chi \text{ (anticlockwise)} \\ \left[-\frac{b}{a}(x_0 - x_i), \frac{a}{b}(y_0 - y_i), 0\right] & \text{if } \gamma > \chi \text{ (clockwise)} \end{cases} \tag{4}$$

Where, γ is the angle between the vector field and the x axis, and χ is the angle between the x axis and the relative position between the obstacle and the UAV. The composite follow-up rotating vector field matrix between the obstacle and the UAV is obtained by superposition of the rotating vector field of two planes:

$$M_i = \begin{cases} \left[\frac{b}{a}(x_0 - x_i), -\frac{a}{b}(y_0 - y_i) - \frac{c}{b}(y_0 - y_i), \frac{c}{b}(y_0 - y_i)\right] & \text{if } \gamma < \chi, \alpha < \beta \\ \left[\frac{b}{a}(x_0 - x_i), -\frac{a}{b}(y_0 - y_i) + \frac{c}{b}(y_0 - y_i), -\frac{b}{c}(z_0 - z_i)\right] & \text{if } \gamma < \chi, \alpha > \beta \\ \left[-\frac{b}{a}(x_0 - x_i), \frac{a}{b}(y_0 - y_i) - \frac{c}{b}(y_0 - y_i), \frac{c}{b}(y_0 - y_i)\right] & \text{if } \gamma > \chi, \alpha < \beta \\ \left[-\frac{b}{a}(x_0 - x_i), \frac{a}{b}(y_0 - y_i) + \frac{c}{b}(y_0 - y_i), -\frac{c}{b}(y_0 - y_i)\right] & \text{if } \gamma > \chi, \alpha > \beta \end{cases} \tag{5}$$

3.3. UAV Position from the Follow-up Rotating Vector Field

In the course of track planning, the UAV will appear shaking phenomenon and flying at a large angle when avoiding obstacles. Therefore, the follow-up rotating vector field with angle adjustment is introduced to make the track meet the requirements of control parameters. The position at the next moment after angle adjustment is presented in Equation 6. The UAV position $\left(\rho_{ix}(k), \rho_{iy}(k), \rho_{iy}(k)\right)$ is obtained due to the effect of the follow-up rotating vector field. κ_s is smoothing coefficient, l is adjustment step length. $\Delta\alpha(k)$ is the deviation of yaw angle in two consecutive sampling times. $\Delta\beta(k)$ is the deviation of flight path angle in two consecutive sampling times. The values of $\Delta\alpha(k)$ and $\Delta\beta(k)$ are related to maximum flight path angle constraint and maximum yaw angle constraint. The maximum angle constraint between two continuous track points is used to limit the angle range. The smoothing coefficient and step length are

introduced to improve the smoothness of path[15].

$$\begin{cases} \rho_i(k+1) = \rho_{ix}(k) + \kappa_s.l.\cos\left(\alpha_{k-1} + \frac{1}{2}|\alpha_k - \alpha_{k-1}|\right) & 0 < |\alpha_k - \alpha_{k-1}| < \Delta\alpha(k) \\ \rho_y(k+1) = \rho_{iy}(k) + \kappa_s.l.\sin\left(\alpha_{k-1} + \frac{1}{2}|\alpha_k - \alpha_{k-1}|\right) & 0 < |\alpha_k - \alpha_{k-1}| < \Delta\alpha(k) \\ \rho_z(k+1) = \rho_{iz}(k) + \kappa_s.l.\cos\left(\beta_{k-1} + \frac{1}{2}|\beta_k - \beta_{k-1}|\right) & 0 < |\beta_k - \beta_{k-1}| < \Delta\beta(k) \end{cases} \tag{6}$$

4. UAV Flight Path Planning Strategies

In this section, two complementary strategies are proposed for computing the UAV's path: avoid collisions based on weighting factors, and track the target.

4.1. Inter-UAVs Artificial Potential Field Strategy with the Collision Avoidance Weighting Factor

In the past works, the artificial potential field method is introduced to deal with the problem of UAV avoiding obstacle. Its basic avoidance idea is that the obstacle produces "repulsion" to the mobile robot. Based on the artificial potential field method, each UAV regards the remaining UAVs as obstacles, and there is a repulsive force between them.

In this paper, we consider that multiple UAVs can reach the same target point. Consequently, the target position of assembling mission position is discussed. Therefore, the mission of track planning corresponds to the fact that all UAVs reach the same target location from different starting points. Supposing there are n UAVs with same model that needs to reach the mission position, $U_{ij}^{rep}(\rho_i)$ is used to represent the potential field between A_i and other UAV, where A_i with $i \in [1, n]$ is the i-th UAV:

$$U_{ij}^{rep}(\rho_i) = \begin{cases} 0 & \text{if } \rho_{ij} \notin S \\ \sum_j^n \eta_i \left\| \frac{1}{\rho_{ij}} - \frac{1}{\rho_0} \right\|_2 \left(\rho_{ig}\right)^{\frac{1}{2}} & \text{if } \rho_{ij} \in S \end{cases} \tag{7}$$

Where, ρ_i refers to the three-dimensional position of the UAV in the global coordinate system. ρ_{ig} refers to the relative position vector from A_i to target. ρ_{ij} refers to the relative position vector from A_i to A_j. In Equation 7, $\|o\|_2$ is L_2 norm of o and η_i is a repulsion factor. S is the scope determined by the distance, $S \in [\rho_{ijmin}, \rho_{ijmax}]$. ρ_{ijmin} is minimum safe distance and ρ_{ijmax} is maximum obstacle avoidance area.

The inter-UAVs potential field force experienced by the UAV is a negative gradient of the potential field. Calculating the potential field force requires obtaining the position information of the UAV through the embedded system. Under normal circumstances, the sensor information of the UAV provides data, especially when this data needs communication with other UAVs, within a certain sampling time. Because there is a high priority to solve the collision avoidance problem, a collision avoidance factor containing distance factors among the UAVs around is introduced. The potential field force between the UAV and each other is therefore as shown in Equation 8.

$$F_i^{rep} = \sum_{j=1, i\neq i}^{n} \frac{\eta_{ij}}{e^{\|\rho_{ij}\|}} \left(\left\| \frac{1}{\rho_{ij}} - \frac{1}{\rho_0} \right\|_2 \left(\rho_{ig}\right)^{\frac{1}{2}} \left(\frac{1}{\rho_{ij}}\right)^2 \nabla\rho_{ij} + \frac{1}{2} \sum_{j=1, j\neq i}^{n} \left\| \frac{1}{\rho_{ij}} - \frac{1}{\rho_0} \right\|_2 \left(\rho_{ig}\right)^{-\frac{1}{2}} \nabla\rho_{ig} \right) \tag{8}$$

Where, η_{ij} is the weight factor between UAV_i and UAV_j is used to represent the collision avoidance priority. By introducing the distance factor $e^{\|\rho_{ij}\|}$, when the distance $\|\rho_{ij}\|$ is far, the influence of UAV_j on UAV_i is small. And, when the distance $\|\rho_{ij}\|$ is relatively close, the influence of UAV_j on UAV_i is greater. Thus, the UAV behavior can

ignore the potential force between to another UAV whe it is far away. In this way, unnecessary collision avoidance behavior is limited, and its impact on the UAV maneuverability is decreased.

4.2. Target tracking strategy

Introducing an attraction potential field from the target, containing relative velocity guides the UAV to reach the target. As shown in Equation 9, $U_i(\rho_i)$ represents the sum of the inter-UAVs potential fields and attraction potential fields, generated from the target. ξ_i is the attraction factor. κ_i is the relative velocity factor between UAV and the target. ρ_{ig} refers to the relative position vector from A_i to the target. And, v_{ig} refers to the relative velocity vector from A_i to the target.

$$U_i(\rho_i) = U_{ig}^{att}(\rho_i) + \sum_{j=1, j\neq i}^{n} U_{ij}^{rep}(\rho_i) = \left(\xi_i \left\|\rho_{ig}\right\| + \kappa_i \left\|v_{ig}\right\|\right) + \sum_{j=1, j\neq i}^{n} U_{ij}^{rep}(\rho_i) \tag{9}$$

Even if, from a theoretic point of view, $U_i(\rho_i)$ is computed from different potential fields, only one vector for each potential field is computed an summed up. This approach, shared by other force-based collision avoidance models, enables to limit the need of computational resources, and may enable the deployment of the collision avoidance behavior on real UAVs.

5. Simulation Experiments

As shown on Fig. 4, a variety of convex polyhedra are used to represent the obstacles. The simulation scenario takes the arrival of four UAVs to the common target, and the initial position of the four UAVs are respectively $(0, 0, 0)$, $(0, 15, 1)$, $(13, 1, 2)$, $(1, 25, 0)$. The initial velocity vector for all the UAVs is $(0.3, 0.3, 0.3)$. The simulation is executed on in the Matlab environment.

Each UAV avoids convex polyhedron obstacles and other UAVs, and has the goal to reach the arrival position. The paths followed by the UAVs are shown on Fig. 4a. Each point corresponds to a step into the simulation process, at which the UAV applies the collision avoidance model. To illustrate the realization of collision avoidance between inter-UAVs and a possible solution to the "dead zone" problem, the top view of the UAV path is drew in Fig. 4b. The problem of "dead zone" appears when the UAV, obstacles and target point are co-linear. In this paper, obstacle avoidance switching strategy is adopted to switch from artificial potential field method to follow-up rotating vector field method. Based on this strategy, the UAV is circling to avoid obstacles instead of stopping in a domain range and failing to follow the path. Consequently, "dead zone" problem should not appear any more.

As shown on Fig. 4a and Fig. 4b, when the UAVs is near the obstacles, the path of UAVs is influenced by the follow-up rotating vector field. After avoiding obstacles, it navigates to the destination by attraction forces. In order to achieve better UAV control effect, the follow-up rotating vector field is computed according to Equation 6 in order to provide smoother path when avoiding obstacles. Collision avoidance between UAVs is shown in Fig. 4c. According to the simulation results, the distance between any two UAVs at any time is greater than a threshold value for ensuring that no collision occurs between UAVs. When the UAVs arrive at the target position, the relative distance becomes low, and below the collision avoidance threshold. As illustrated on Fig. 4c, the distance oscillates because the UAVs are moving around the target position and avoiding collision with the nearby UAVs.

On Fig. 5, yaw angle and flight path angle of three-dimensional flight track are shown. The values for the simulation parameters are detailled in Table 1. The new angle curve on Fig. 5 adds a smoothing strategy under the simulation conditions. After the introduction of the follow-up rotating vector field with smoothing processing, the angle range of UAV is reduced during obstacles avoidance. UAV3 without smoothing strategy started to generate "jitter" (immediate rotation, oscillation) effect at $t = 30s$, heading angle variation range is close to 180°. After combining the smoothing strategy with the rotating vector field, when UAV3 avoids obstacles, the phenomenon of "jitter" weaken and provides good input conditions for UAVs tracking control. ON Fig. 5b, the change range of the flight path angle curve with

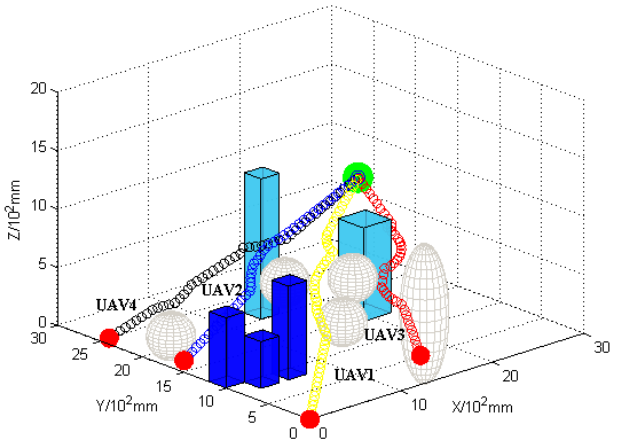

(a) Multi-UAVs global track map

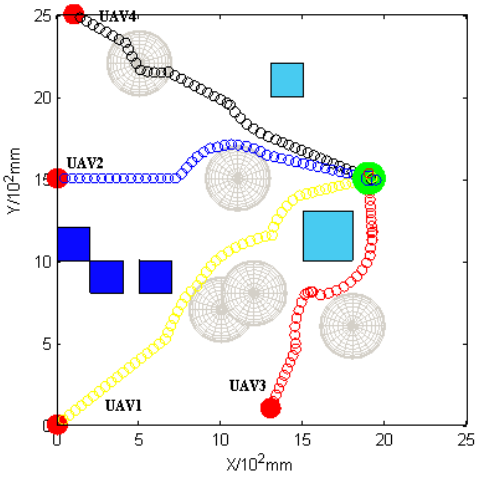

(b) Track top view

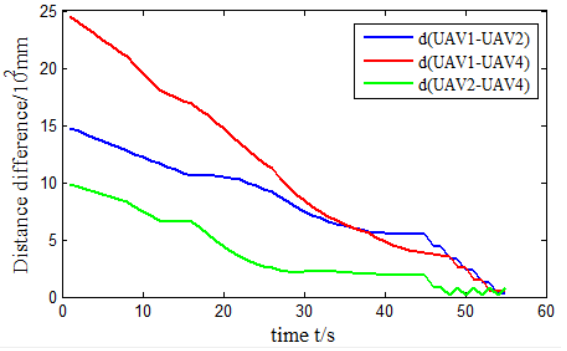

(c) Relative distance between UAVs

Fig. 4. Complex 3D environment simulation

Table 1. Simulation Parameters

Parameters		Parameters	
Maximum yaw angle$^{(rad)}$	0.7	Maximum flight path angle$^{(rad)}$	0.7
Smoothing coefficient κ_s	0.4	Adjustment step $^{10^2}$ mm	0.5

smoothing strategy is narrowed to avoid the need to provide a large lift in flight and improve the UAV climbing performance.

6. Conclusion

UAV path planning not only needs to avoid collision between UAVs, but also needs to avoid the other obstacles. In this paper, an obstacle avoidance method based on a follow-up rotating vector field is introduced to realize obstacle avoidance of UAV when they have the same target position. The collision avoidance weighting factor is introduced

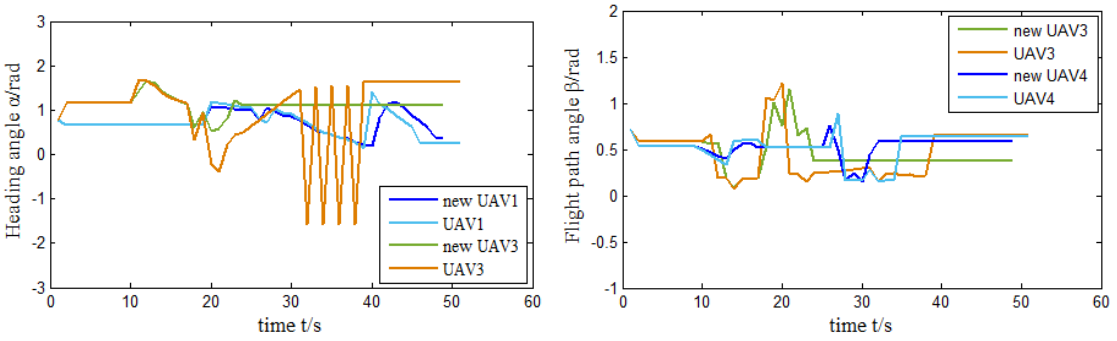

(a) Heading angle comparison

(b) Flight path angle comparison

Fig. 5. Angle Simulation

to complete collision avoidance between inter-UAVs. In addition, the follow-up rotating vector field and smoothing strategy are combined to obtain a better path to reduce the "jitter" phenomenon.This paper focuses on the strategy algorithm of UAV avoiding obstacles or other obstacles, solves the dead zone problem in the previous algorithm, and obtains a smooth and optimized UAV trajectory. Simulation results verify the effectiveness of the follow-up rotation vector field, and show that the algorithm can realize simultaneous planning of UAV collision avoidance, and solve the problem of "dead zone" and "jitter" effect, which can better adapt to the trajectory planning of UAV in complex environment.

One perspective of this work is to include communication mechanisms among the UAVs in order to exchange up-to-date positions as fast as possible. A second perspective is to implement the proposed model with the SARL[1] agent programming language, and deploy them on the associated UAV simulator.

References

[1] Van den Berg, J., Guy, S.J., Lin, M., Manocha, D., 2011. Reciprocal n-body collision avoidance, in: Pradalier, C., Siegwart, R., Hirzinger, G. (Eds.), Robotics Research: The 14th International Symposium ISRR, Springer Tracts in Advanced Robotics, Springer-Verlag. pp. 3–19.

[2] Van den Berg, J., Lin, M., Manocha, D., 2008. Reciprocal velocity obstacles for real-time multi-agent navigation, in: Robotics and Automation, 2008. ICRA 2008. IEEE International Conference on, pp. 1928–1935. doi:10.1109/ROBOT.2008.4543489.

[3] Buisson, J., Galland, S., Gaud, N., Yasar, Gonçalves, M., Koukam, A., 2013. Real-time collision avoidance for pedestrian and bicyclist simulation: a smooth and predictive approach, in: the 2nd International Workshop on Agent-based Mobility, Traffic and Transportation Models, Methodologies and Applications (ABMTRANS), Procedia Computer Science, Elsevier, Halifax, Nova Scotia, Canada.

[4] Guy, S., Chhugani, J., Kim, C., Satish, N., Lin, M., Manocha, D., Dubey, P., 2009. ClearPath: Highly parallel collision avoidance for multi-agent simulation, in: ACM SIGGRAPH/Eurographics Symposium on Computer Animation (SCA).

[5] Helbing, D., Molnar, P., 1997. Self-organization phenomena in pedestrian crowds. Self-organization of complex structures: from individual to collective dynamics , 569–577.

[6] Hwang, Y.K., Ahuja, N., 1992. A potential field approach to path planning. IEEE Transactions on Robotics and Automation 8, 23–32.

[7] Koenig, S., Likhachev, M., 2005. Fast replanning for navigation in unknown terrain. Robotics, IEEE Transactions on 21, 354–363. doi:10.1109/TRO.2004.838026.

[8] Lewin, K., 1951. Social fields (social forces). Field Theory in Social Science .

[9] Mualla, Y., Najjar, A., Daoud, A., Galland, S., Nicolle, C., Yasar, A.u.h., Shakshuki, E., 2019. Agent-based simulation of unmanned aerial vehicles in civilian applications: A systematic literature review and research directions. Future Generation Computer Systems (FGCS) 100, 344–364. doi:10.1016/j.future.2019.04.051.

[10] Reynolds, C., 1999. Steering behaviors for autonomous characters, in: Proceedings of the Game Developers Conference, p. 763–782.

[11] Teal Group, 2018. World Unmanned Aerial Vehicle Systems – 2018 Market Profile and Forecast. Technical Report. Teal Group Corporation.

[12] Treiber, M., Hennecke, A., Helbing, D., 2000. Congested traffic states in empirical observations and microscopic simulations. Phys. Rev. E 62, 1805–1824. URL: http://link.aps.org/doi/10.1103/PhysRevE.62.1805, doi:10.1103/PhysRevE.62.1805.

[13] Treuille, A., Cooper, S., Popović, Z., 2006. Continuum crowds. ACM Trans. Graph. 25, 1160–1168.

[1] http://www.sarl.io